

MICROSCOPIC CHARACTERIZATION OF THE NANOSTRUCTURE OF POLYACRYLONITRILE BASED FIBER CROSS SECTIONS

Christina Kunzmann¹, Maria Luiza Basílio Graça Couto¹, Judith Moosburger-Will² and Siegfried Horn^{1,2}

¹ Experimental Physics II, Institute of Physics, University of Augsburg, 86135 Augsburg, Germany
Email: Christina.kunzmann@physik.uni-augsburg.de, Web Page: <http://www.physik.uni-augsburg.de/de/exp2/>

²Institute of Materials Resource Management, University of Augsburg, 86135 Augsburg, Germany
Web Page: <https://www.mrm.uni-augsburg.de/>

Keywords: PAN fibers, nanopores, surface structure, volume structure

Abstract

The present work addresses the nanoscale structure of technical Polyacrylonitrile fibers, which are precursor fibers for the production of high tensile strength carbon fibers. Surface and volume structure of the fibers were analyzed by atomic force microscopy. Use of an extra sharp tip guarantees a lateral resolution of about 2 nm. The analysis demonstrates the existence of nanoscale pores, both on the fiber surface and in the fiber volume. The size of the pores in the volume is slightly smaller compared to that on the surface. While the nanoporous surface structures show a preferred orientation along the fiber axis, the nanopores in the fiber bulk are distributed isotropically within the fiber cross section.

1. Introduction

Polyacrylonitrile (PAN) is the most widely used precursor material for carbon fiber production [1, 2]. The PAN fiber tow, composed out of several thousand single fibers, is produced using a wet spinning process [3]. PAN solution is pumped through a spinneret into a liquid coagulation bath, where it becomes thermodynamically unstable and decomposes in two phases [4, 5]. The polymer-rich phase forms the bulk of the fibers, while the solvent-rich phase develops into voids [6, 7]. The two-phase arrangement is called gel network structure [7]. During the subsequent stretching and washing steps, the polymer-rich phase of this network is oriented along the stretching direction (fiber axis) and forms the typical fibrils [8]. It was shown, that the parameters of the coagulation bath, e.g. temperature and concentration, have a significant influence on the structure of the PAN fibers [5, 9, 10]. To allow textile processing of the PAN fibers during the subsequent processing steps, a polymeric textile finish is applied on the fiber surface.

The properties of the PAN precursor fiber, e.g. its micro- and nanostructure, are closely linked to the performance of the corresponding carbon fiber [3, 11]. Investigation of the nanostructure of fibers along the complete process chain is one important approach to obtain a fundamental understanding of process induced structural changes and their influence on fiber properties. Atomic force microscopy (AFM) allows a non-destructive nanoscale characterization of the surface of carbon fibers as well as of non-conducting PAN fibers [12–15]. The lateral resolution sensitively depends on the geometry and durability of the tip used [16–18]. In recent years newly developed technologies enable the production of tips with high aspect ratio and small diameter. Such tips allow precise measurements of nanoscale structures [19].

Using such super sharp AFM probes we demonstrated in earlier work that wet-spun PAN fibers are characterized by a nanoporous surface structure [19, 20]. We showed that this surface structure is

conserved along the whole process chain and also exists on the surface of the corresponding carbon fibers [19, 21, 22]. In order to investigate if these nanopores are only characteristic for the fiber surface or also a property of the bulk fiber, in the actual work we analyze the volume structure of technical PAN fibers by nanoscale AFM investigation of fiber cross sections.

2. Experimental

To remove the textile finish, technical PAN fibers were cleaned in a 0.1 M/L solution of Tetrabutylammonium fluoride trihydrate (TBAF, ACROS organics, 90 %) in Tetrahydrofuran (THF, Sigma Aldrich, $\geq 99.9\%$) for 18 h at room temperature. Afterwards, the fibers were stirred for 2 h at room temperature in Methanol, rinsed in 2-Propanol and dried at room temperature.

Cross sections of the PAN fibers were prepared by embedding the fibers in resin and cutting it at room temperature perpendicular to the fiber axis by an ultramicrotome using a diamond knife.

The AFM measurements were performed using a Bruker Dimension ICON in tapping mode with two different probes. TESPAs from Bruker with a tip radius of 8 nm were used for fiber surface images with a scan size of $5\ \mu\text{m} \times 5\ \mu\text{m}$ and a resolution of 512 pixels \times 512 pixels. The evaluation of the nanoroughness was based on nine AFM images and calculated using the method of Jäger et al. with a symmetric baseline and a cut-off 0.7 [23].

Super sharp EBD-SSS NCHR AFM probes from Nanotools with a tip radius of 2 nm were used for scan sizes of $500\ \text{nm} \times 500\ \text{nm}$ on the surface and for all images of the cross sections. The scanning resolution of these images was 512 pixels \times 512 pixels.

The images were processed using the software Nanoscope Analysis v1.40.

3. Results and discussions

3.1 Nanoscale AFM investigation of PAN fiber surface

In order to analyze the nanoscale surface structure of technical PAN fibers the textile finish was removed from the fiber surface. The cleaning process was controlled by investigation of the nanoroughness R_a using TESPAs. While the nanoroughness of the original surface coated by the finish is typically below 1 nm – here $(0.8 \pm 0.3)\ \text{nm}$ – the values of the nanoroughness of the cleaned PAN fiber surface is $(1.3 \pm 0.3)\ \text{nm}$. The coverage of the nanoscale surface structure of the PAN fibers by the finish is removed, resulting in the increased nanoroughness of the cleaned fibers.

The technical PAN fibers offer a fibrillar surface structure (see height and phase images of size $5\ \mu\text{m} \times 5\ \mu\text{m}$ in Figure 1a and 1b), which is well orientated along the fiber axis. Thin fibrils form groups and result in thicker fibrils. The thin fibrils have an average width of $(52 \pm 17)\ \text{nm}$, the fibril groups have a mean width of $(180 \pm 48)\ \text{nm}$.

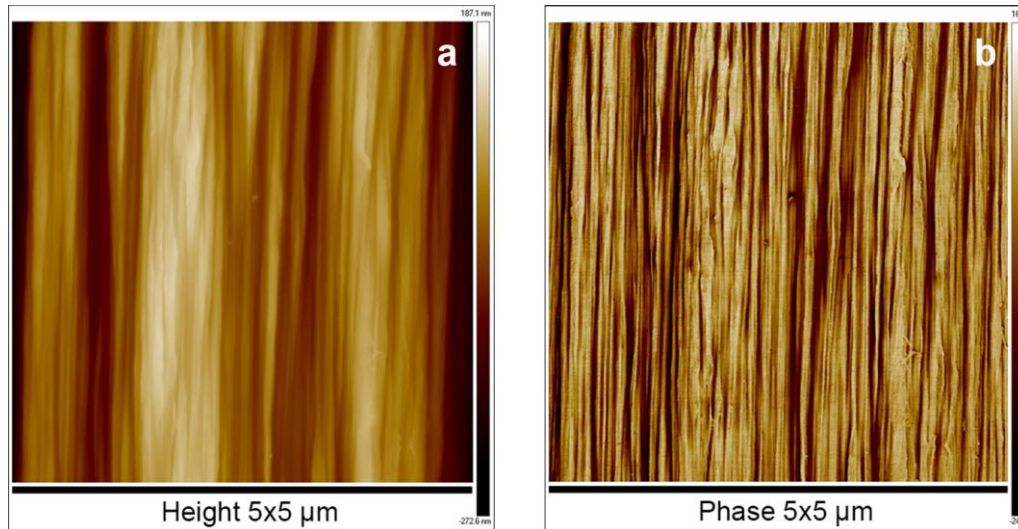


Figure 1. AFM height (a) and phase (b) image of the fibrillar surface structure of technical PAN fibers.

A higher resolution image of the fiber surface structure of size 500 nm x 500 nm is shown in Figure 2 a and b (use of EBD-SSS NCHR probes). The height and phase images reveal an additional structure on top of the fibrils, which is formed by open, almost circular nanoscale pores. These pores exist on the complete fiber surface. The pores have a mean width of (11.7 ± 2.9) nm. They are separated by thin intersections of (3.3 ± 2.1) nm width. The histogram in Figure 3 shows an unimodal, almost symmetric distribution of the pore width. At several positions the pores arrange anisotropically along the fiber axis and sometimes are connected to chain-like structures. We assume that these chains are formed by merging of nanopores during the stretching of the PAN fibers during the production process. As the nanoporous surface structure is found for all investigated regions, it is assumed to be an intrinsic property of the PAN fiber surface.

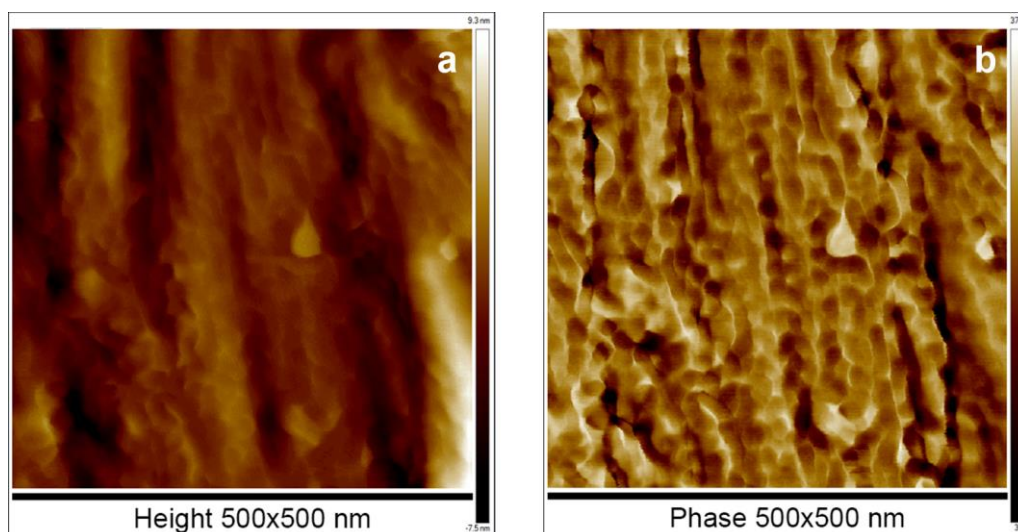


Figure 2. AFM height (a) and phase (b) images of the surface of a technical PAN fiber scanned with super sharp probe.

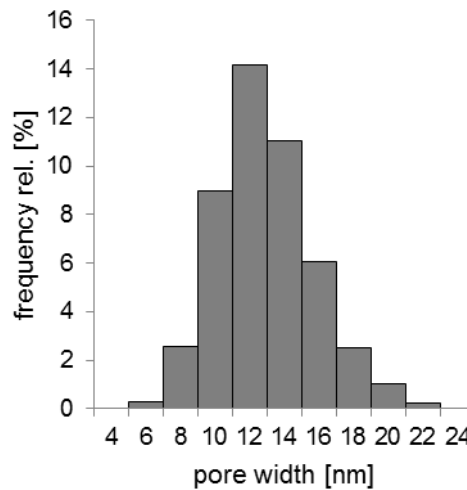


Figure 3. Histogram of width distribution of the nanopores of the surface of a technical PAN fiber.

3.2 Nanoscale AFM investigation of PAN fiber volume

Figure 4 (a, b) shows AFM height and phase images of size $10\mu\text{m} \times 10\mu\text{m}$ including the cross section of the technical PAN fiber, scanned using an EBD-SSS probe. The embedded fiber is clearly visible and can be distinguished from the surrounding resin. In order to analyze the nanoscale bulk structure of the fiber, AFM height and phase images of size $500\text{nm} \times 500\text{nm}$ were measured. Figure 5 (a, b) represent a zoom into the skin area of the fiber, i.e. in a region of the fiber cross section close to the fiber-resin border. Again, a nanoporous structure is found. The almost circular nanopores have an average width of (9.4 ± 2.9) nm, which is slightly smaller than the size of the nanopores on the surface. The histogram in Figure 5a shows an unimodal, almost symmetrical width distribution of the pores. A homogeneous distribution is observed. In contrast to the surface structure no preferred orientation is found. Each pore is surrounded by polymeric material, so that a closed porosity in the original fiber can be assumed.

A pore structure on nanoscale is also found in the center of the fiber cross section (see Figure 5c, d). The pores in the fiber center have the same isotropic arrangement as in the skin region. Evaluation of the pore size results in an average width of (8.6 ± 2.7) nm, which is slightly smaller than the pore width in the skin region and clearly smaller than that on the fiber surface (see Table 2). Thus, a slight trend to smaller pore size exists comparing the skin of the fiber to the center, reflecting a radial gradient. However, as the variation of the pore width is high, the pore widths of all three investigated regions of the PAN fiber (surface, skin region of bulk, central region of bulk) coincide within the margins of error.

In contrast to the surface structure, no clear fibrillar structures can be identified on the cross sections of fiber skin and center. The isotropically distributed nanopores do not indicate an arrangement to fibrils or the existence of fibril boundaries and of inter-fibrillar regions.

Based on the presented results the nanoporous structure, found for all investigated regions of the fiber cross sections, is assumed to be an intrinsic property of the PAN fiber.

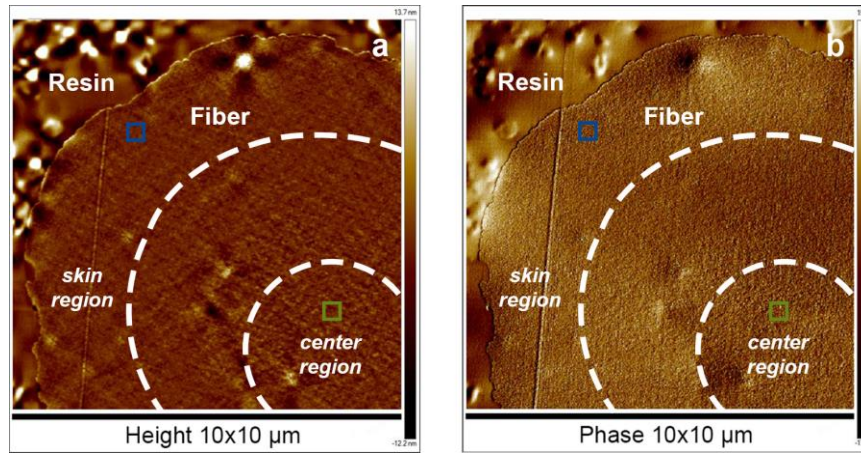


Figure 4. AFM height (a) and phase (b) images of the cross section of a technical PAN fiber.

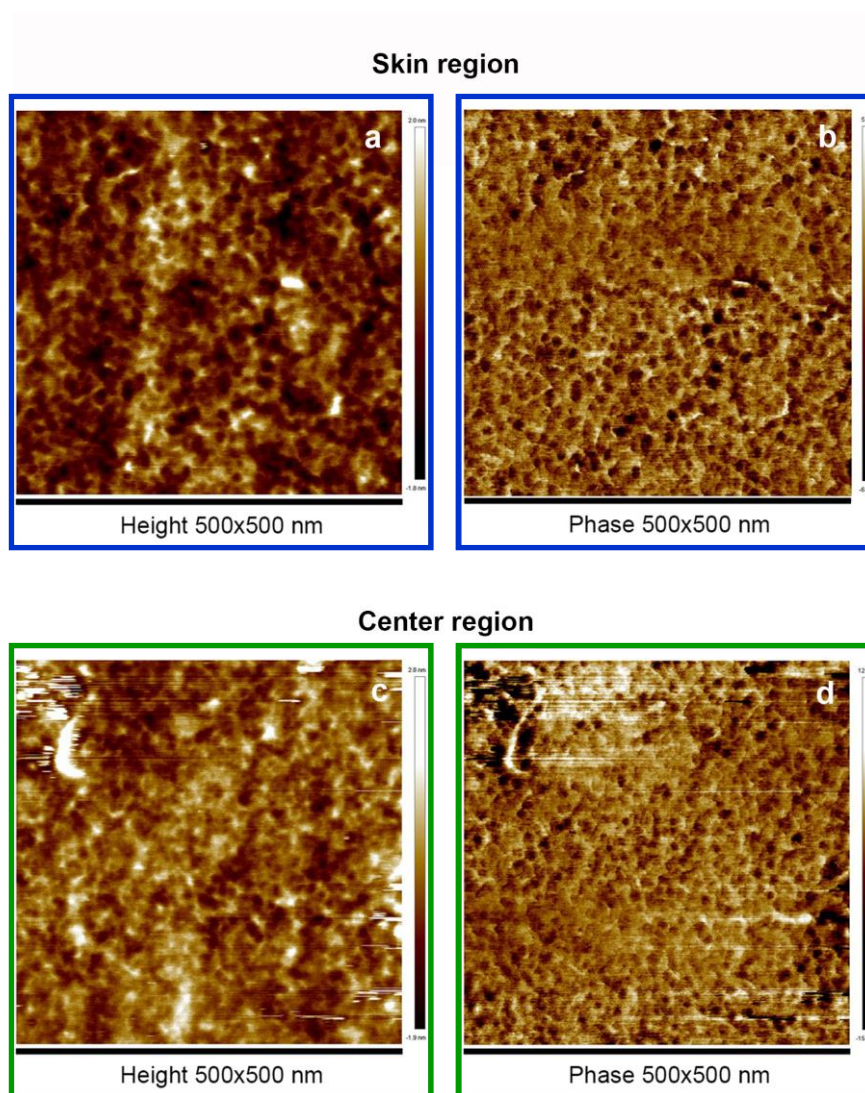


Figure 5. AFM height (a, c) and phase (b, d) images of the cross section of a technical PAN fiber scanned with super sharp probe. The images (a, b) are from the skin region and (c, d) from the center of a PAN fiber.

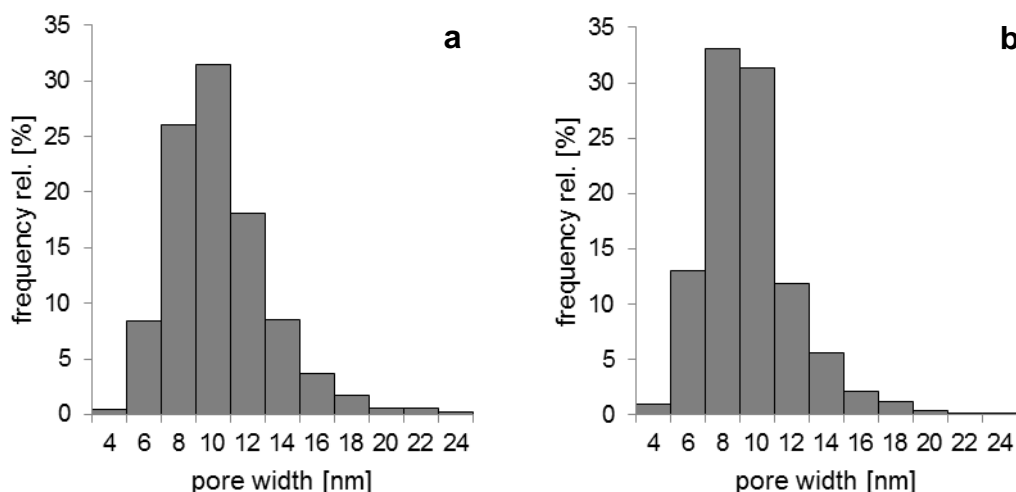


Figure 6. Width distribution of the nanopores of a technical PAN fiber (a) from the skin region and (b) from the center of the fiber cross section.

Table 2. Nanopore width of a technical PAN fiber on the surface and in the volume.

	fiber surface	fiber volume: skin area	fiber volume: central area
<i>pore width</i> (nm)	11.67 ± 2.98	9.35 ± 2.98	8.55 ± 2.67

4. Conclusions

We have investigated the surface and bulk nanostructure of technical PAN fibers by AFM. A nanoporous structure is detected, both on the surface and in the bulk of the fibers. The open pores on the surface are arranged along the fiber axis and are partially merged to chain-like structures. In contrast, the closed pores in the volume are arranged isotropically and with no obvious preferred orientation. A slight trend of decreasing pore size from the skin region to the center region of the fibers is observed. In contrast to the fiber surface, no clear fibrillar structures can be identified in the fiber volume.

References

- [1] K. Morita, Y. Murata, A. Ishitani, K. Murayama, T. Ono, A. Nakajima. Characterization of commercially available PAN (polyacrylonitrile)-based carbon fibers. *Pure Appl Chem* 3, 58, 1986.
- [2] S. Damodaran, P. Desai, A.S. Abhiraman. Chemical and Physical Aspects of the Formation of Carbon Fibres from PAN-based Precursors. *The Journal of The Textile Institute* 4, 81: 384–420, 2008.
- [3] C. Wilms, G.H. Seide, T. Gries. The relationship between process technology, structure development and fibre properties in modern carbon fibre production. *Chem Eng Trans*, 32: 1609–14, 2013.
- [4] J.W. Cahn. Phase Separation by Spinodal Decomposition in Isotropic Systems. *J Chem Phys* 1, 42: 93, 1965.

- [5] S. Arbab, P. Noorpanah, N. Mohammadi, M. Soleimani. Designing index of void structure and tensile properties in wet-spun polyacrylonitrile (PAN) fiber. I. Effect of dope polymer or nonsolvent concentration. *J Appl Polym Sci* 6, 109: 3461–9, 2008.
- [6] J.P. Bell, J.H. Dumbleton. Changes in the Structure of Wet-Spun Acrylic Fibers During Processing. *Text Res J* 3, 41: 196–203, 1971.
- [7] P. van de Witte, P.J. Dijkstra, J. van den Berg, J. Feijen. Phase separation processes in polymer solutions in relation to membrane formation. *J Membrane Sci* 1-2, 117: 1–31, 1996.
- [8] J.P. Craig, J.P. Knudsen, V.F. Holland. Characterization of Acrylic Fiber Structure. *Text Res J* 6, 32: 435–48, 1962.
- [9] J.P. Knudsen. The Influence of Coagulation Variables on the Structure and Physical Properties of an Acrylic Fiber. *Text Res J* 1, 33: 13–20, 1963.
- [10] P. Bajaj, Surya Kumari Munuktla, A.A. Vaidya, D.C. Gupta. Influence of Spinning Dope Additives and Spin Bath Temperature on the Structure and Physical Properties of Acrylic Fibers. *Text Res J* 10, 59: 601–8, 1989.
- [11] E. Fitzer, W. Frohs. Modern carbon fibres from polyacrylonitrile (PAN)-polyheteroaromatics with preferred orientation. *Chem Eng Technol* 1, 13: 41–9, 1990.
- [12] S.N. Magonov. Surface Characterization of Materials at Ambient Conditions by Scanning Tunneling Microscopy (STM) and Atomic Force Microscopy (AFM). *Appl Spec Rev* 1-2, 28: 1–121, 1993.
- [13] G. Binnig, C. Gerber, E. Stoll, T.R. Albrecht, C.F. Quate. Atomic Resolution with Atomic Force Microscope. *Europhys Lett* 12, 3: 1281–6, 1987.
- [14] Q. Zhong, D. Inniss, K. Kjoller, V.B. Elings. Fractured polymer/silica fiber surface studied by tapping mode atomic force microscopy. *Surf Sci Lett* 1-2, 290: L688-L692, 1993.
- [15] Á.S. Paulo, R. García. Unifying theory of tapping-mode atomic-force microscopy. *Phys Rev B* 4, 66, 2002.
- [16] D.J. Keller, C. Chih-Chung. Imaging steep, high structures by scanning force microscopy with electron beam deposited tips. *Surf Sci* 1-3, 268: 333–9, 1992.
- [17] C. Bustamante, D. Keller, G. Yang. Scanning force microscopy of nucleic acids and nucleoprotein assemblies. *Curr Opin Struc Biol* 3, 3: 363–72, 1993.
- [18] A. Engel, C.-A. Schoenenberger, D.J. Müller. High resolution imaging of native biological sample surfaces using scanning probe microscopy. *Curr Opin Struc Biol* 2, 7: 279–84, 1997.
- [19] C. Kunzmann, J. Moosburger-Will, S. Horn. High-resolution imaging of the nanostructured surface of polyacrylonitrile-based fibers. *J Mater Sci* 21, 51: 9638–48, 2016.
- [20] C. Kunzmann, T. Peter, J. Moosburger-Will, S. Horn. Microscopic Surface Characterization of Technical and Textile Polyacrylonitrile Fibers. *Proceeding at the 17th European Conference on Composite Materials, Munich*, 2016.
- [21] J. Moosburger-Will, E. Lachner, M. Löffler, C. Kunzmann, M. Greisel, K. Ruhland, S. Horn. Adhesion of carbon fibers to amine hardened epoxy resin: Influence of ammonia plasma functionalization of carbon fibers. *Applied Surface Science*, 453: 141–52, 2018.
- [22] J. Moosburger-Will, J. Jäger, J. Strauch, M. Bauer, S. Strobl, F.F. Linscheid, S. Horn. Interphase formation and fiber matrix adhesion in carbon fiber reinforced epoxy resin: Influence of carbon fiber surface chemistry. *Composite Interfaces* 7, 24: 691–710, 2016.
- [23] J. Jäger, J. Moosburger-Will, S. Horn. Determination of nano-roughness of carbon fibers by atomic force microscopy. *J Mater Sci* 19, 48: 6803–10, 2013.